



Radix Rehmanniae Extract Ameliorates Experimental Autoimmune Encephalomyelitis by Suppressing Macrophage-Derived Nitrate Damage

Wenting Li¹, Hao Wu¹, Chong Gao¹, Dan Yang², Depo Yang³ and Jiangang Shen^{1*}

¹ LKS Faculty of Medicine, School of Chinese Medicine, The University of Hong Kong, Hong Kong, Hong Kong, ² Department of Chemistry, The University of Hong Kong, Hong Kong, Hong Kong, ³ School of Pharmaceutical Sciences, Sun Yat-sen University, Guangzhou, China

OPEN ACCESS

Edited by:

Feng Chen,
Augusta University, United States

Reviewed by:

Marcos Lopez,
Fundación Cardiovascular de
Colombia, Colombia
Deepesh Pandey,
Johns Hopkins University,
United States

*Correspondence:

Jiangang Shen
shenjg@hkucc.hku.hk

Specialty section:

This article was submitted to
Oxidant Physiology,
a section of the journal
Frontiers in Physiology

Received: 27 February 2018

Accepted: 18 June 2018

Published: 20 July 2018

Citation:

Li W, Wu H, Gao C, Yang D, Yang D
and Shen J (2018) Radix Rehmanniae
Extract Ameliorates Experimental
Autoimmune Encephalomyelitis by
Suppressing Macrophage-Derived
Nitrate Damage.
Front. Physiol. 9:864.
doi: 10.3389/fphys.2018.00864

Multiple sclerosis (MS) is a neuroinflammatory disease in central nervous system (CNS) without effective treatment or medication yet. With high prevalence of MS patients worldwide and poor therapeutic outcome, seeking novel therapeutic strategy for MS is timely important. *Radix Rehmanniae* (RR), a typical Chinese Medicinal herb, has been used for neuroinflammatory diseases in Traditional Chinese Medicine for centuries. However, scientific evidence and underlying mechanisms of RR for MS are unclear. In this study, we tested the hypothesis that RR could attenuate the progress and severity of MS via suppressing macrophage-derived nitrate damage and inflammation by using experimental autoimmune encephalomyelitis (EAE) model for mimicking MS pathology. The results showed the RR treatment effectively ameliorated clinical disease severity, inhibited inflammation/demyelination in spinal cord, and alleviated CNS infiltration of encephalitogenic T cells and activated macrophages. Meanwhile, RR possessed bioactivities of scavenging ONOO⁻ and reducing the expression of iNOS and NADPH oxidases in the spinal cords of the EAE mice. Furthermore, RR treatment suppressed nuclear factor- κ B (NF- κ B) signaling pathway in the splenocytes of EAE mice. The *in vitro* experiments on macrophages and neuronal cells exerted consistent results with the *in vivo* animal experiments. Taken together, we conclude that *Radix Rehmanniae* extract has therapeutic values for ameliorating EAE/MS pathological process and disease severity and its underlying mechanisms are associated with anti-inflammation and inhibiting macrophage-derived nitrate damages. Further study could yield novel promising therapeutic agent for multiple sclerosis.

Keywords: *Radix Rehmanniae*, multiple sclerosis, macrophage, nitrate damage, (NF- κ B) signaling pathway

INTRODUCTION

Multiple sclerosis (MS) is an inflammatory auto-immune disease characterized by focal demyelination, axonal and neuronal damage in central nerve systems (CNS) (Thompson et al., 2010). Currently, immunomodulation and immunosuppression are the major therapeutic strategies for MS but carry severe side effects. With the prevalence of 2.5 million MS

patients worldwide and poor therapeutic outcome, the majority of MS patients eventually develop into handicap. Seeking novel therapeutic strategy for MS is timely important. Experimental autoimmune encephalomyelitis (EAE) is a widely adopted animal model mimicking the key features of MS, including CNS-directed leukocyte infiltrations and inflammatory microenvironment induction, which destroy CNS structures and result in progressive paralysis (Lassmann and van Horssen, 2011). EAE animal model provides a reliable tool not only for understanding the mechanisms of MS but also for drug discovery.

Free radicals, including reactive oxygen species (ROS) and reactive nitrogen species (RNS), are intimately associated with MS pathogenesis. Oxidative stress-mediated CNS damages have been found both in both MS patients as well as EAE animal model (Cross et al., 1997; Smith et al., 1999). Both oligodendrocytes and neurons are highly vulnerable to oxidative/nitrative damage (Jack et al., 2007; Bishop et al., 2009). Excessive ROS/RNS derived from macrophage triggers oxidative damages, aggravates demyelination, axonal degradation, and neuronal cell death (Dunham et al., 2017). As a representative RNS, peroxynitrite (ONOO^-) is rapidly produced by the reaction of superoxide ($\text{O}_2^{\bullet-}$) and nitric oxide (NO). ONOO^- exerts strongly membrane penetrability and highly cytotoxicity to CNS. Both human adult CNS-derived oligodendrocytes and motor neurons are highly susceptible to ONOO^- -mediated injury (Li et al., 2011; Nikić et al., 2011). Increased 3-nitrotyrosine (3-NT), a footprint marker of ONOO^- , was identified in the oligodendrocytes of the MS samples featured oligodendrocytes death (Jack et al., 2007). Acute and chronic relapsing pathogenesis of EAE was ameliorated by the treatment of 5,10,15,20-tetrakis (4-sulfonatophenyl) porphyrinatoiron (III) chloride (FeTPPS), a representative peroxynitrite decomposition catalyst (PDC) (Bolton et al., 2008). Furthermore, MS patients had low level of uric acid, an ONOO^- scavenger, in serum and CSF associated with disease activity or treatment response (Dujmovic et al., 2009). Therefore, targeting ONOO^- could be an important therapeutic strategy for EAE or MS.

Traditional Chinese medicine (TCM) has been used for neurodegenerative diseases including MS (Liu et al., 2012). *Radix Rehmanniae* (RR), is one of the most frequent used herbal items in TCM formulas for MS patients (Song et al., 2017). RR exerts various bioactivities such as anti-osteoporotic (Oh et al., 2003), anti-inflammatory (Kim et al., 1999; Lau et al., 2009), immunomodulatory (Kim et al., 1998; Sung et al., 2011) and neuroprotective effects (Yu et al., 2006; Lee et al., 2011). The neuroprotective effects of RR could be attributed to the properties of antioxidant and anti-inflammations (Tian et al., 2006). RR attenuated the cisplatin-induced damage in HEI-OC1 auditory cells and the underlying mechanisms could be attributed to its antioxidant properties by inhibiting lipid peroxidation and scavenging free radicals, including superoxide radical, hydroxyl radical, and hydrogen peroxide (Yu et al., 2006). However, direct evidence about the neuroprotective effects of RR for MS or EAE is still lack. In the present study, we tested the hypothesis that RR could attenuate neuroinflammation and demyelination in EAE via inhibiting the infiltration of encephalitogenic T cells

and activated macrophages and preventing ONOO^- -mediated neurotoxicity.

MATERIALS AND METHODS

Reagents

Radix Rehmanniae was purchased from KANG MEI Pharmaceutical Co., Ltd (Guangdong, China). Mouse myelin oligodendrocytes glycoprotein (35-55) peptide (MOG₃₅₋₅₅, MEVGWYRSPFSRVVHLYRNGK) with the purity of over 96% (wt/wt) was purchased from Chinese Peptide Company (Zhejiang, China), incomplete Freund's adjuvant from Sigma-Aldrich (St. Louis, MO, USA), Mycobacterium tuberculosis H37RA from BD Biosciences (Difco, BD) and *Pertussis Toxin* from List Biological Laboratories (CA, USA). Percoll gradient was purchased from GE Healthcare Life Sciences (Pittsburgh, PA, USA). Cell surface-staining antibodies obtained from eBioscience (San Diego, CA, USA), including CD45-PE (30-F11), CD3e-FITC (145-2C11), CD4-Pacific Blue (RM4-5), and CD11b-APC (M1/70). Primary antibodies for 3-NT and iNOS were obtained from Abcam (Cambridge, UK); Bax, p-p65^{Ser536}, p65, p-IKK α/β ^{Ser176/180}, IKK β , p-I κ B α ^{Ser32}, I κ B α , and GAPDH from Cell signaling Technology (Beverly, USA); p47^{phox} and p67^{phox} from Santa Cruz (Dallas, TX, USA). For HPLC analysis, all solvents used were of HPLC-grade. Catalpol with over 98% purity was purchased from Shanghai Tauto Biotech. Co., Ltd (Shanghai, China). ONOO^- donor 3-morpholiniosydnonimine (SIN-1) was purchased from Cayman Chemical (Ann Arbor, MI, USA), Lipopolysaccharides (LPS) from *Escherichia coli* O111:B4 was purchased from Sigma-Aldrich. HKYellow-AM, an ONOO^- selective probe, were obtained from Professor Yang Dan's laboratory (Chemical Biology, HKU, HK).

Preparation of RR Extract

The dried RR materials were cut into small pieces (about $0.2 \times 0.2 \times 0.2$ cm). The sliced samples (400.0 g) were macerated overnight and repeatedly ultrasonic-extracted with 80% ethanol/water (3×4 L) for 40 min each time. Then, the extracted solutions were evaporated under vacuum (30°C) to remove ethanol and remaining aqueous were frozen and freeze-dried to obtain RR extract powder (162.8 g). The procedure of the RR extraction was restrictively standardized for the quality consistence.

Qualitative Analysis

To characterize the chemical profile of RR, LCMS-IT-TOF (Shimadzu, Kyoto, Japan) was adopted. The system equipped with a SIL-20AC auto-injector, two LC-20AD pumps, a CTO-20A column oven, a SPD-M20A DAD and an electrospray ionization (ESI) interface. Mass spectrometric analysis was performed with QIT coupled to TOF mass spectrometer.

Chromatographic separations were achieved on an AQ-C18 column ($5 \mu\text{m}$, 4.6×250 mm, ACE, Scotland). The chromatographic conditions were as follows: flow rate of 0.8 mL/min, sample injection volume of $10 \mu\text{L}$, column temperature of 25°C and mobile phase A (0.1% formic acid-water) and mobile phase B (acetonitrile). The gradient profile was optimized as the

following: 0–10 min, 1% B; 10–20 min, 1–2% B; 20–25 min, 2–5% B; 25–55 min, 5–15% B; 55–65 min, 15–25% B; 65–80 min, 25–45% B; 80–85 min, 45–70% B; 85–90 min, 70–90% B.

The electrospray source of the MS was operated in positive/negative ion modes and the operating parameters were: nebulizing gas flow rate, 1.5 L/min; the heated capillary temperature, 200°C; CDL temperature, 200°C; capillary voltage, 4,000 V; detector TOF voltage, 1,600 V. Full scan mass spectra were acquired from m/z 100 to m/z 1,000 Da with accurate mass measurement of all mass peaks. The data were processed and analyzed by LCMS solution Software Version 3.0 (Shimadzu, Kyoto, Japan).

Quantitative Analysis

Catalpol has been reported to ameliorate the pathological process of EAE mice (Yang et al., 2017; Li et al., 2018). Thus, we selected Catalpol as mark compound for quantitative quality control of RR. Catalpol was determined at 210 nm wavelength using UHPLC UltiMate 3000 (Thermo Fisher Scientific, USA). The chromatographic conditions were the same with qualitative experiment described as previous. RR extract powder was accurately weighed, dissolved in 70% MeOH by sonication and filtrated through 0.45 µm filter for quantitative analysis.

For validation of the quantitative methodology, linearity, sensitivity, precision, accuracy, and stability were detected as previous described (Liu et al., 2013). Briefly, stock solution (1 mg/mL) of Catalpol was prepared in 50% MeOH. Six concentrations of Catalpol stander were analyzed in triplicates in HPLC to prepare calibration curves. Accuracy and precision were evaluated by measuring the intra-day and inter-day variabilities and recovery of standard compounds. Stability was conducted by analyzing RR extract over a period of 2, 4, 6, 8, 12, and 24 h. The limits of detection (LOD) and limits of quantitation (LOQ) under the present conditions were determined at an S/N (signal/noise) of about 3 and 10, respectively. The data were monitored, recorded and analyzed by Chromeleon Version 7.2 (Thermo, USA).

Animals

Female C57BL/6N mice (8–10 week old) were obtained from the Laboratory Animal Unit, the University of Hong Kong. All animal care and experimental procedures were approved by the University Committee on the Use of Live Animals in Teaching and Research (CULATR). The mice were housed in the pathogen free environment with 12 h dark/light cycles.

EAE Induction and Treatment

Female C57BL/6N mice were immunized for active induction of EAE as our previous described (Wu et al., 2016). Briefly, the mice were subcutaneously injected with 200 µg MOG35–55 in complete Freund's adjuvant containing 5 mg/ml heat killed *Mycobacterium tuberculosis H37RA*. *Pertussis Toxin* (200 ng) was injected intravenously twice on 0 and 2 days post-immunization (dpi). Body weights and clinical scores were measured daily. To evaluate clinical severity, EAE symptoms were scored as follows: 0, no clinical signs; 0.5, partially limp tail; 1, paralyzed tail; 1.5, hindlimb paresis or loss in coordinated movement; 2, loss in

coordinated movement and hindlimb paresis; 2.5, one hindlimb paralyzed; 3, both hindlimbs paralyzed; 4, hindlimbs paralyzed, weakness in forelimbs; 5, forelimbs paralyzed.

For drug administration, the dosage of RR was determined according to the equivalent dose of mice to human subjects (60 g crude drug/ 60 kg). RR extract powder was dissolved in 0.3% (wt/vol) sodium carboxymethyl cellulose (CMC-Na) in saline. RR extract (3.7 g/kg/day) were orally administrated into the EAE mice on daily basis starting at 2 dpi for prevention protocol or 11 dpi for treatment protocol. The vehicle and normal groups were treated with an equal volume of 0.3% CMC-Na saline as control.

Cell Lines

Human neuroblastoma SH-SY5Y cells and mouse RAW264.7 macrophages were purchased from American Type Culture Collection (ATCC, Manassas, VA). Cells were cultured in high glucose Dulbecco's Modified Eagle Medium (DMEM) with 10% heat-inactivated fetal bovine serum (FBS, Gibco), 1% penicillin/streptomycin (PS, Gibco) and 1% 2 mM L-glutamine (Gibco). For subculture, SH-SY5Y cells were collected by trypsin digestion and RAW264.7 cells by using sterile cell scraper (Corning, USA) and passaged at a split ratio of 1:10.

Cellular Experiments

SH-SY5Y cells were used to test the ONOO⁻ scavenging capability of RR and the cells were exposed to ONOO⁻ donor SIN-1. Briefly, the SH-SY5Y cells were seeded onto 6-well plates at a density of 5×10^5 cells/well and incubated with 500 µM SIN-1 for 1 h. In the RR group, the cells were treated with 50 µg/mL of RR extract for 1 h prior to SIN-1 challenge or treated with PBS as control group.

To evaluate the anti-inflammation effects of RR, RAW264.7 macrophages were activated by lipopolysaccharide (LPS). Cells were seeded onto 6-well plates at a density of 5×10^5 cells/well and challenged with LPS (1 µg/mL) for 30 min. In the RR group, the cells were pre-incubated with 50 µg/ml RR extract for 1 h prior to LPS exposure. The medium was collected as conditioned medium (CM) for the following experiments.

MTT Assay

Cell viability as detected with 3-(4,5-dimethylthiazol-2-yl)-2,5-diphenyltetrazolium bromide (MTT) assay according to the manufacturer's instruction. SH-SY5Y cells at a density of 5×10^4 cells/well were cultured at 37°C under 5% CO₂ atmosphere for 24 h and then incubated with MTT (0.5 mg/mL) for 4 h at 37°C. The medium was removed and 150 µl DMSO was added into each well. The absorbance at 490 nm was measured by Multi-plate Reader (Model 680, Bio-Rad). Cell viability was calculated by the absorbance values and normalized to control.

ONOO⁻ Assessment

HKYellow-AM is our newly developed ONOO⁻ fluorescent probe with high sensitivity and selectivity (Gong et al., 2015; Peng et al., 2016). We detected ONOO⁻ production both *in vivo* and *in vitro* experiments. For *in vivo* study, the mice at 18 dpi were intravenously injected with HKYellow-AM (10 µM,

1 mL/kg) at 15 min before sacrificed. After perfused with PBS, the fresh L4-L6 spinal cords were immediately dissected, embedded into O.T.C., cut into 30 μ m sections, counterstained the nucleus with DAPI and imaged by a confocal laser scanning microscope LSM 780 at the conditions of excitation wavelength of 543 nm and emission wavelength of 567 nm. For *in vitro* study, cells were stained with 10 μ M HKYellow-AM for 30 min and washed with PBS. The fluorescent images were captured by Carl Zeiss fluorescent microscope equipped with Axio Vision digital imaging system.

Western Blot Analysis

The proteins of tissues or cells were extracted by using radioimmunoprecipitation assay (RIPA) buffer containing 1% proteinase and phosphatase inhibitor cocktails (Sigma-Aldrich). Protein lysates were separated by 11% sodium dodecyl sulfate-polyacrylamide (SDS-PAGE) gel electrophoresis, transferred onto polyvinylidene fluoride (PVDF) membrane, and separately immunoblotted with primary antibodies including 3-NT (1:1000), iNOS (1:1000), p47^{phox} (1:1000), p67^{phox} (1:1000), p-p65^{Ser536} (1:1000), p65 (1:1000), p-IKK α / β ^{Ser176/180} (1:1000), IKK β (1:1000), p-I κ B α ^{Ser32} (1:1000), I κ B α (1:1000) and GAPDH (1:2000) following HRP-conjugated secondary antibodies (1:2000). The signals were detected by chemiluminescent ECL Select Kit (GE Healthcare, IL, USA), captured by Gel-Doc system (Bio-Rad, CA, USA) and analyzed by Image Lab software (Bio-Rad, CA, USA).

Histopathology

Mice were perfused with PBS and then fixed with 4% paraformaldehyde (PFA). Isolated L4-L6 spinal cords were post-fixed in 4% PFA overnight at 4°C, dehydrated in gradient ethanol, permeabilized with xylene, embedded into paraffin and cut into 5 μ m sections. Slides were stained with H&E or Luxol fast blue (LFB) for assessment of inflammation and demyelination, respectively. Inflammation and demyelination were scored as described previously (Li et al., 2010a). Briefly, inflammation was scored as follows: 0, none; 1, a few inflammatory cells; 2, organization of perivascular infiltrates; and 3, increasing severity of perivascular cuffing with extension into the adjacent tissue; Demyelination was scored as follows: 0, none; 1, rare foci; 2, a few areas of demyelination; and 3, large (confluent) areas of demyelination.

Immunofluorescence

For immunofluorescence *in vivo*, post-fixed brains and spinal cord were immersed in 30% sucrose solution at 4°C for complete dehydration, embedded in O.C.T and cut into 30 μ m sections. Sections were co-stained with primary antibodies CD3 (1:400) and CD11b (1:400). For *in vitro* immunofluorescence, cells were seeded onto 12 mm glass coverslips. After different experiment, cells were fixed in 4% PFA for 20 min and stained with primary antibodies p65 (1:400). After washed by PBS, the sections or cells were stained with fluorochrome conjugated secondary antibodies, counterstained the nucleus with DAPI and mounted with antifade medium. Immunofluorescent images

were captured by a confocal laser scanning microscope LSM 800 (Carl Zeiss).

Flow Cytometry

Mice were sacrificed at 30 dpi. Spleen, brain and spinal cord tissues were dissected out, homogenized and suspended into single-cells. Mononuclear cells (MNCs) were harvested using density based Percoll gradient centrifugation. The isolated MNCs were stained with surface markers, CD45-PE, CD3e-FITC, CD4-Pacific Blue, and CD11b-Alexa700. Flow cytometric analysis was performed on FACS LSR II (BD Biosciences, CA, USA) and data were analyzed with FlowJo software (Treestar, Ashland, OR).

Statistical Analysis

Data were expressed as the Mean \pm SEM. Statistical analysis was assessed by using unpaired Student's *t*-test for two group designed comparisons or one-way ANOVA followed by Dunnett's multiple-comparison test for multiple group comparisons. All analyses were performed using GraphPad Prism Version 6.0 software (GraphPad Software Inc., CA, USA). $p < 0.05$ was considered as statistical significance.

RESULTS

Qualitative and Quantitative Analysis of RR

For quality control study, we identified the chemical ingredients of RR extract by LCMS-IT-TOF. Chromatographic condition was optimized and a well-separated fingerprint was obtained (Figure 1A). In both positive- and negative- ion models, a total of 24 compounds were identified by comparing their UV spectra, matching diagnostic ions and fragmentation pathways with reference compounds (Li et al., 2010b; Xu et al., 2013) (Figures 1B,C). As shown in Table 1, the structures and fragment ions of identified compounds were summarized. The identified compounds in the RR extract were iridoid glycosides and phenethylalcohol glycosides, 12 of which were iridoid glycosides (1, 2, 4-10, 12, 15, and 21), 8 of which were phenethylalcohol glycosides (11, 14, 16-20, and 22). Others were triterpenoids or phenolic acids.

We further quantitatively analyzed Catalpol as a bioactive compound in RR. HPLC was used to verify the terms of linearity, LOD, LOQ, precision, accuracy, and stability. The linearity of standard curve was $y = 0.0337x + 6.7212$ with correlation coefficients (r) 0.9999. LOD and LOQ of all analytes were 0.1025 μ g/mL and 0.3413 μ g/mL, respectively. Precision was assayed by intra- and inter-day variations (RSDs) at three concentrations of analytes in triplicate, which were 1.02 and 2.31% respectively. The analytical method had the accuracy with the overall recovery of 97.8–101.4%. For stability assay, RSD of peak areas for Catalpol within 24 h was 0.32%. These results suggest that HPLC-DAD method has good sensitivity, accuracy, and stability. The validated HPLC-DAD method was subsequently applied to measure the content of Catalpol, with the concentration of 4.32 mg/g in RR samples.

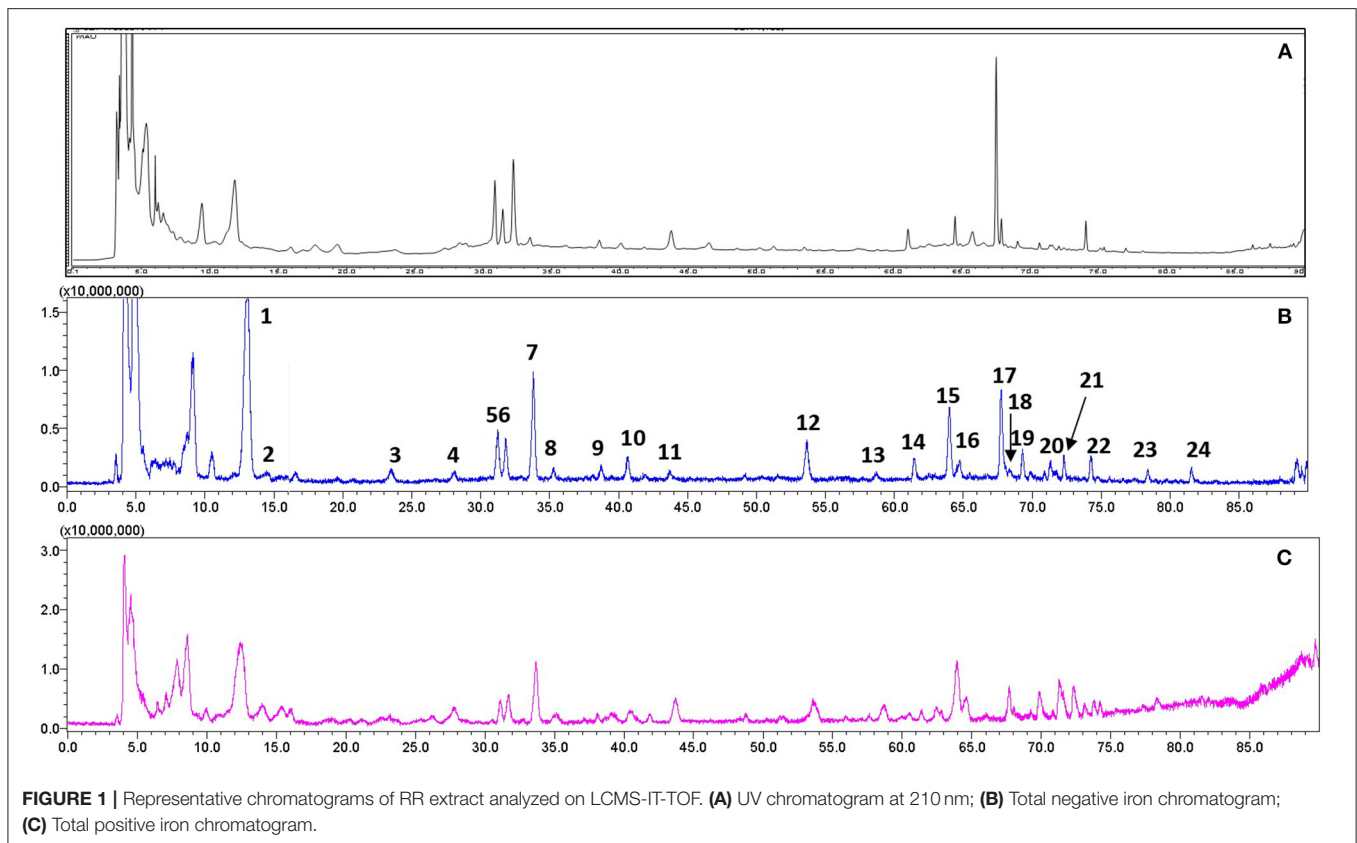


FIGURE 1 | Representative chromatograms of RR extract analyzed on LCMS-IT-TOF. **(A)** UV chromatogram at 210 nm; **(B)** Total negative iron chromatogram; **(C)** Total positive iron chromatogram.

RR Alleviates EAE Progression

We then investigated the anti-inflammatory effects of RR on the EAE model. RR extract at dosage of 3.7 g/kg/day was orally administered to the mice. For the prophylactic protocol, RR treatment was started at 2 dpi. RR treatment significantly decreased daily and accumulative clinical scores in EAE mice compared with vehicle group ($P < 0.01$, **Figures 2A,B**). Meanwhile, RR effectively attenuated EAE progression, reduced EAE symptom severity ($P < 0.01$) and delayed disease onset ($P < 0.05$) (**Table 2**). For therapeutic protocol, RR treatment was started at the time of disease onset (11 dpi). Similarly, RR treatment group showed lower daily clinical scores than vehicle control group, especially at chronic phase (25–30 dpi) (**Figure 2C**). Moreover, RR treatment starting at 11 dpi also showed to attenuate disease severity evidenced by the mean maximal and accumulative clinical scores ($P < 0.05$, **Figure 2D**, **Table 2**). Thus, the results indicate that RR could alleviate the disease severity and progress of EAE as a prophylactic agent or therapeutic strategy. To mimic clinical therapeutic situation, further study was conducted by using treatment protocol in following EAE experiments.

RR Reduces Inflammation and Demyelination in Spinal Cords of EAE Mice

We then investigated the neuroprotective effects of RR on EAE-induced CNS pathology. After the EAE mice received RR with treatment protocol at 30 dpi, the sections of lumbar

spinal cords were detected by H&E and LFB staining. As shown in **Figures 2E,F**, compared with EAE mice with vehicle treatment, the RR treated EAE mice had significant lower scores of inflammatory infiltrations and smaller demyelinating areas ($P < 0.05$, **Figure 2G**). The results indicate that RR could attenuate CNS demyelination and inflammation in EAE mice.

RR Decreases Populations of CD3⁺ and CD11b⁺ Cells in Spinal Cords and Brains of EAE Mice

We next investigated different populations of the inflammatory cells between vehicle and RR treated EAE mice. Mononuclear cells (MNCs) from brains and spinal cords of EAE mice at 30 dpi (treatment protocol) were isolated and analyzed by using flow cytometry. The surface expressions of CD3, CD4, and CD11b were investigated to identify T-cell and macrophages/microglia infiltration in the lesions. Compared with vehicle EAE mice, RR treatment mice had dramatically decreased rates of CD3⁺ T cells and CD11b⁺ CD45^{high} macrophages in both spinal cord and brain tissues ($P < 0.01$, **Figures 3A–C**). In addition, immunofluorescence results further revealed that RR-treated mice had a smaller number of infiltrated CD3⁺ T cells and CD11b⁺ macrophages in cerebral parenchyma and the white matter of spinal cord (**Figure 3D**).

TABLE 1 | Compounds identified in RR extract.

Peak no.	Retention time (min)	[M-H] ⁻	[M+HCOO] ⁻	(-) ESI-MS (m/z) Main fragment ions	Formula	Identification
1	13.04	361.1158	407.1190	361.1139; 199.0627; 169.0500; 384.9359; 248.9609; 154.9788	C ₁₅ H ₂₂ O ₁₀	Catalpol
2	14.56	397.0922	443.0969	365.1044; 316.9483; 297.1224	C ₁₅ H ₂₃ ClO ₁₀	Glutinoside
3	23.50	397.0943	443.0945	341.1098; 316.9469; 226.9778; 112.9907	C ₂₈ H ₁₄ O ₃	2-(Dibenzo[ghi,mno]fluoranthren-1-ylcarbonyl) benzoic acid
4	27.99	361.1171		326.1234; 316.9459; 112.9856	C ₁₅ H ₂₂ O ₁₀	Danmelittoside
5	31.37	685.2181	731.2267	384.92297; 248.9549; 263.0779; 341.1154; 248.9606; 505.1471; 685.2161	C ₂₇ H ₄₂ O ₂₀	Rehmannioside D
6	31.69	435.2243	389.1928	319.0780; 183.1034; 215.0819; 112.9959	C ₂₀ H ₃₆ O ₁₀	Rehmaionoside A/Rehmaionoside B
7	33.70	523.1702	569.1709	523.1702; 463.1343	C ₂₁ H ₃₂ O ₁₅	Melittoside
8	35.22	345.1554		367.1360; 265.1019; 165.0924; 248.9601; 154.9789	C ₁₆ H ₂₆ O ₈	Rehmapicroside
9	38.68	347.1311	393.1404	347.1351; 167.0743; 149.0667; 248.9611; 154.9769; 248.9596; 154.9770; 329.1333	C ₁₅ H ₂₄ O ₉	Leonuride or isomer
10	40.60	373.1148		318.7710; 316.9545; 248.9636; 113.0061	C ₁₆ H ₂₂ O ₁₀	Geniposidic acid
11	43.63	461.1664		315.1091; 397.1125; 204.963; 154.9775	C ₂₀ H ₃₀ O ₁₂	Decaffeoyl-verbascoside
12	53.55	375.1295		213.0715; 169.0923; 103.9678; 131.7047; 191.0681	C ₁₆ H ₂₄ O ₁₀	8-Epiloganic acid
13	58.85	451.2147		391.0532; 293.0553; 277.0559; 226.9850; 129.1799	C ₂₇ H ₃₂ O ₆	28-Deoxonimbolide
14	61.54	785.2529		623.2172; 461.1685; 315.1005; 477.1517; 703.1626; 541.1231	C ₃₅ H ₄₆ O ₂₀	Purpureaside C/Echinacoside
15	64.11	389.2192	435.2237	389.2192; 161.0542; 179.0726; 248.9595; 154.9754; 316.9467; 248.9457	C ₂₀ H ₃₆ O ₁₀	Rehmaionoside A/Rehmaionoside B
16	64.78	799.2666		623.2188; 461.1619; 248.9573; 703.1678; 557.0945; 384.9435; 384.9355	C ₃₆ H ₄₈ O ₂₀	Cistanoside A/Jionoside A1/Jionoside A2
17	67.75	623.1975		461.1660; 384.9374; 315.1066; 315.1115; 248.9595; 154.9775	C ₂₉ H ₃₆ O ₁₅	Acteoside
18	68.12	813.2823		637.2318; 623.2012; 461.1617; 659.2773; 513.2349	C ₃₇ H ₅₀ O ₂₀	Jionoside B1/Jionoside B2
19	69.21	623.1973		461.1660; 384.9380; 315.1153	C ₂₉ H ₃₆ O ₁₅	Isoacteoside/Forsythoside A
20	70.89	637.2136		461.1669; 452.9183; 248.9533; 316.9483	C ₃₀ H ₃₈ O ₁₅	Jionoside D/Leucosceptoside A/Leucosceptoside
21	72.29	523.1822		452.9175; 316.9470; 248.9533; 193.0507; 162.0315; 154.9770	C ₂₅ H ₃₂ O ₁₂	6-O-E-Feruloylajugol
22	74.25	651.2309		457.1848; 384.9551; 520.9061; 383.9357; 248.9616; 313.1651; 237.1449	C ₃₁ H ₄₀ O ₁₅	Martynoside/Martynoside isomer
23	78.48	535.2542		452.9211; 349.1507; 238.7846; 248.9545; 112.9959	C ₂₈ H ₄₀ O ₁₀	Strophanthidin arabinoside
24	77.89	329.2324		313.1670; 267.1626; 211.1375; 171.0987	C ₁₈ H ₃₄ O ₅	Octadecenoic acid

RR Reduces ONOO⁻ Level in Spinal Cords of EAE Mice

We then detected the effects of RR extract on scavenging ONOO⁻ and inhibiting tyrosine nitration in the spinal cords of EAE mice by using HKYellow-AM probe and measuring 3-NT expression respectively. HKYellow-AM is a highly selective ONOO⁻ probe and used for detecting ONOO⁻ in different experimental systems (Gong et al., 2015; Peng et al., 2016). EAE mice were received RR treatment starting at 11 dpi for treatment protocol and the spinal cords were collected at 18 dpi. Fluorescent imaging study revealed that the vehicle EAE

mice had remarkably increased HKYellow-AM-positive staining fluorescence, indicating the increased ONOO⁻ production in the section of the spinal cords. Compared with vehicle EAE mice, the RR treated mice showed much less ONOO⁻-positive fluorescence staining cells in the spinal cords (**Figure 4A**). The expression of 3-NT was also detected with western blot analysis. Consistently, EAE vehicle mice had a significantly higher expression of 3-NT in the spinal cords at 18 dpi than normal control group. The RR treatment EAE mice had remarkably decreased the expression of 3-NT in the spinal cords than the vehicle treated EAE mice (**Figure 4B**). In addition, the

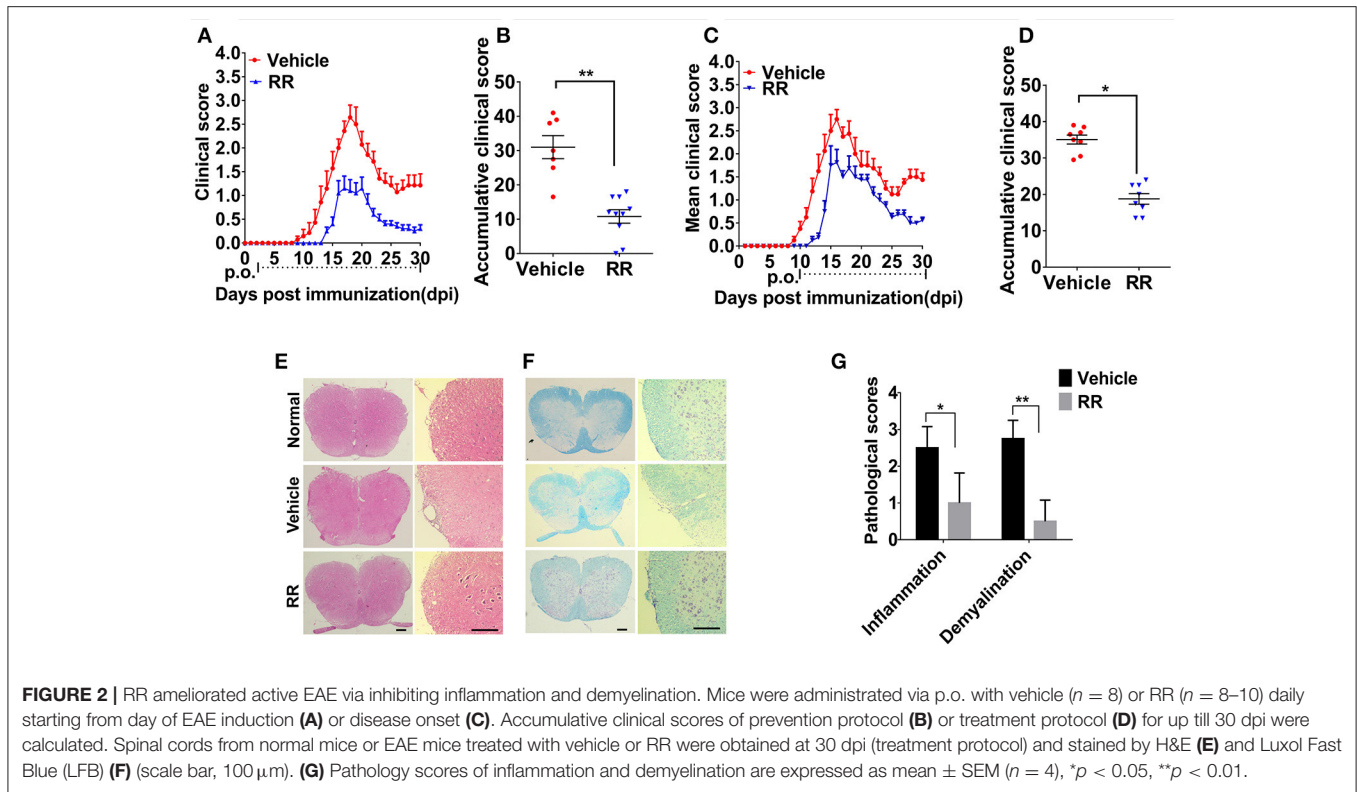


TABLE 2 | Clinical features of EAE in mice in the administration of vehicle or RR.

Group	Treatment protocol		Preventive protocol		
	Incidence (%)	Mean maximal score	Incidence (%)	Mean maximal score	Average day of onset
Vehicle	100	3.38 \pm 0.23	100	3.07 \pm 0.189	12.29 \pm 0.79
RR	100	2.44 \pm 0.68*	90	1.72 \pm 0.22**	14.89 \pm 0.35*

Mean \pm SEM * $P < 0.05$, ** $P < 0.01$.

expressions of iNOS and NADPH oxidase subunit p47^{phox}, and p67^{phox} were detected by using western blot analysis. The vehicle treated EAE mice had the higher expression levels of iNOS, p47^{phox}, and p67^{phox} in spinal cords than the normal control mice, which were reversed in the RR treated EAE mice (Figure 4C). These results suggest that RR not only has ONOO⁻ scavenging effects but also inhibit the expression of iNOS and NADPH oxidases, subsequently reducing the production of ONOO⁻ in the EAE pathology.

RR Inhibits NF- κ B Signaling in the Splenocytes of EAE Mice

Transcription factor NF- κ B is a crucial signaling regulating ROS/RNS production involved in the inflammatory process of EAE (Mc Guire et al., 2013). In MS/EAE, though activating NF- κ B pathway, activated macrophages induces the production of proinflammatory cytokines, including ROS and NO (Glass et al., 2010). ROS/RNS reversely activate NF- κ B pathway in the loop positive-feedback inflammatory process (Zhang et al., 2016). Thus, we detected the effects of RR regulating NF- κ B signaling

for suppressing macrophage-derived ROS/RNS production. Splenocytes, dominated by macrophages and lymphocyte, were isolated from the spleens of the normal, vehicle-, or RR-treated EAE mice with treatment protocol at 18 dpi. The expression of phosphorylated IKK α/β , I κ B α , and p65 were detected by western blot analysis. The vehicle-treated EAE mice revealed the increased expressions of the phosphorylated IKK α/β , I κ B α , and p65 in comparison with the normal control mice, which were significantly reduced in the RR treated EAE mice (Figure 5A). These results indicate that RR could inhibit NF- κ B signaling in the EAE mice.

RR Inhibits Expressions of iNOS, NADPH Oxidases, and NF- κ B Signaling in LPS-Activated RAW264.7. Macrophages

We then tested the effects of RR on the expressions of iNOS, NADPH oxidases and NF- κ B signaling in the LPS-stimulated mouse RAW264.7 macrophages. LPS activates NF- κ B signaling and induces the expressions of iNOS and NADPH oxidases to generate ROS/RNS, subsequently mediating

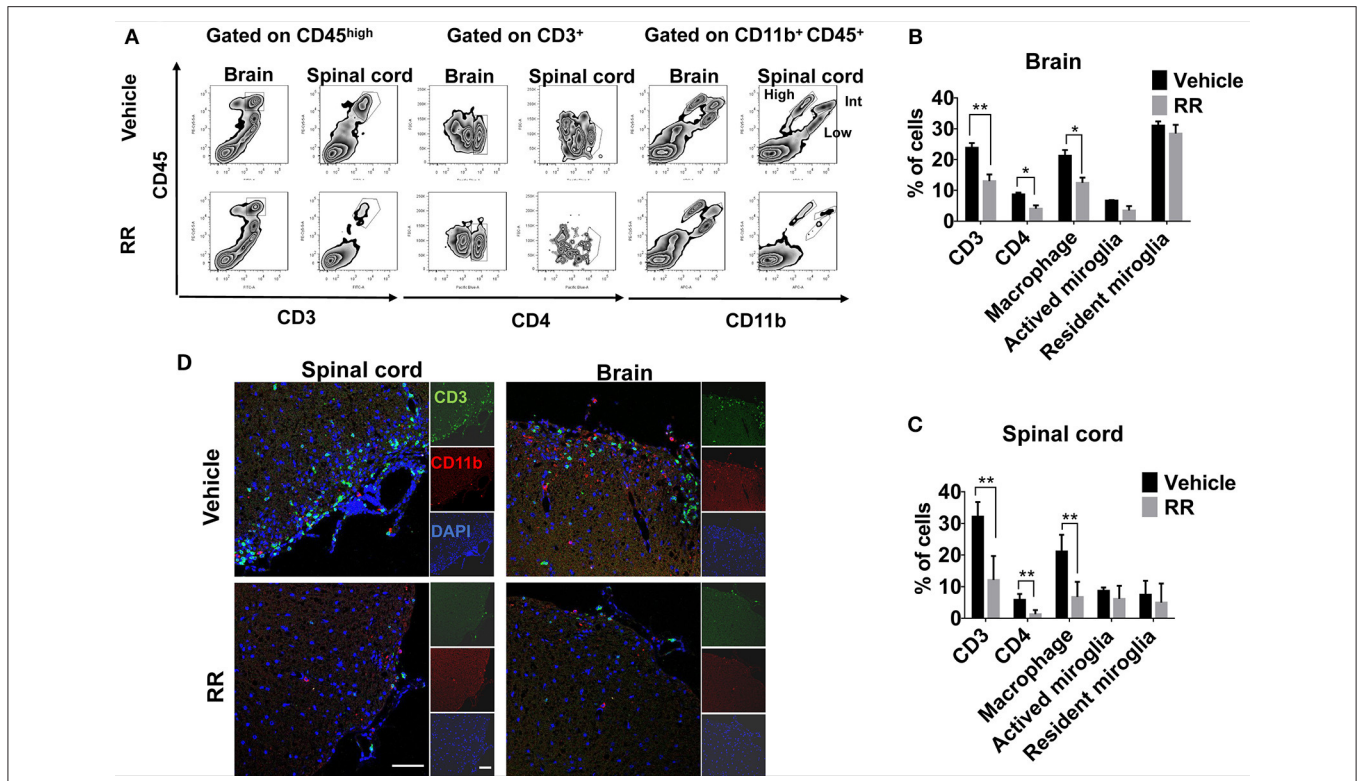


FIGURE 3 | RR decreased the populations of CD3⁺ and CD11b⁺ cells in active EAE. MNCs were isolated from brain or spinal cord in RR or vehicle-treated EAE mice at 30 dpi (treatment protocol). **(A)** Cells were analyzed for expression of CD3 or CD4 in the lymphocyte gate and that of CD11b in total MNC gate by flow cytometry. CD11b⁺ CD45^{high} cell was defined as macrophage, CD11b⁺ CD45^{int} as active microglia and CD11b⁺ CD45^{low} as resident microglia. Percentages of positive cells in brain **(B)** or spinal cord **(C)** are represented (*n* = 4). **(D)** Immunofluorescent co-staining of CD3⁺ (green) and CD11b⁺ (red) cells with nucleus (blue) in spinal cord (left) and brain (near choroid plexus within lateral ventricle, right) at 30 dpi (scale bar, 50 μm). **P* < 0.05, ***P* < 0.01.

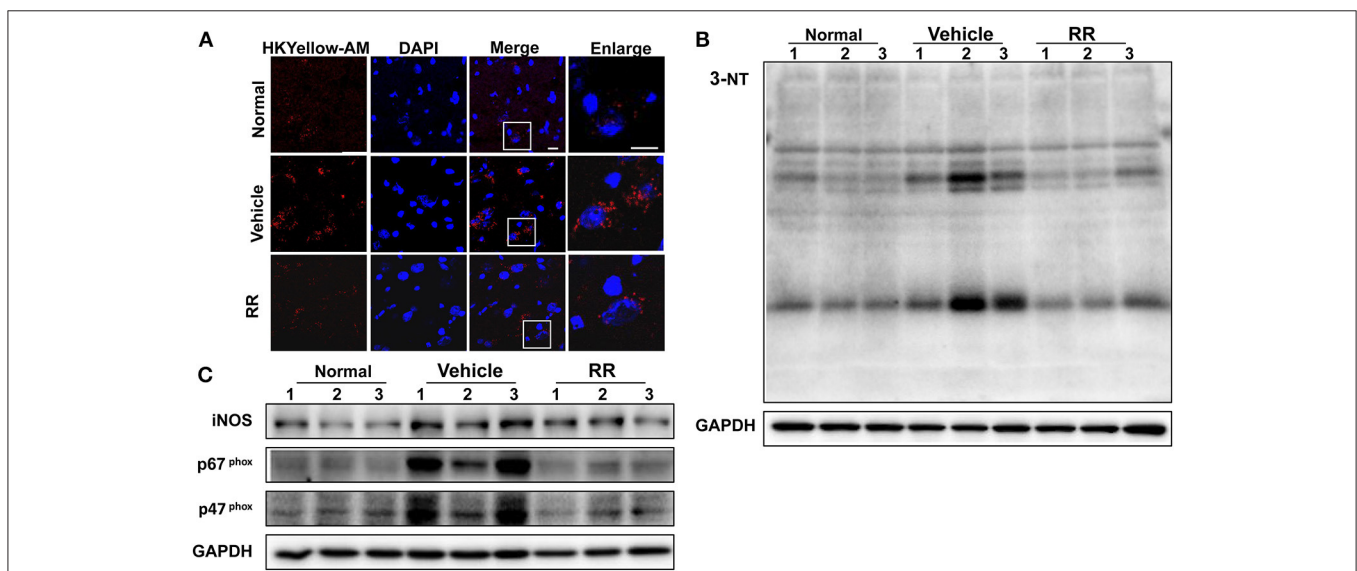


FIGURE 4 | RR reduced ONOO⁻ production in active EAE spinal cord. Spinal cords in normal mice and RR or vehicle-treated EAE mice (*n* = 3) at 18 dpi (treatment protocol) were obtained. ONOO⁻ levels were detected using HKYelllow-AM probe. **(A)** The immunofluorescent images of HKYelllow-AM (red) and nucleus (blue) in spinal cord at 18 dpi (scale bar, 10 μm). Western blotting was conducted to analyze the expression of 3-NT **(B)** and iNOS, p67^{phox}, p47^{phox} **(C)**.

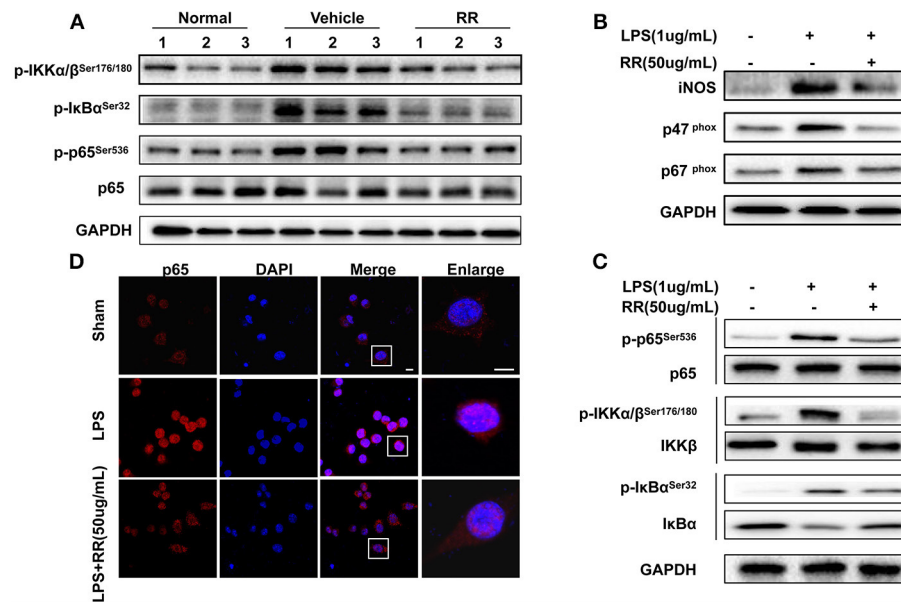


FIGURE 5 | RR suppressed ONOO⁻ generation by inhibiting NF-κB signaling both *in vivo* and *in vitro*. **(A)** Splenocytes from normal, RR-, or vehicle-treated EAE mice ($n = 3$) at 18 dpi (treatment protocol) were analyzed for the expression of p65 and phosphorylated IKKα/β, IκBα and p65 by western blot assay. Macrophage cell line, RAW264.7 was pre-incubated with RR (50 μg/mL) or sham for 1 h prior to LPS (1 μg/mL) challenge for 30 min **(B–D)**. Western blotting was conducted to analyze the expressions of iNOS, p67^{phox}, p47^{phox} **(B)** and NF-κB signaling-associated proteins **(C)**. The nuclear translocation of p65 was examined by immunofluorescent staining **(D)**. Scale bar represented 5 μm.

nitritative stress (Xie et al., 1994). As shown in **Figure 5B**, the expressions of iNOS, p47^{phox} and p67^{phox} in the macrophages were significantly up-regulated by LPS stimulation, which were reversed by RR treatment. Moreover, LPS stimulation induced the phosphorylation of IKK/IκBα/p65 but inhibited the expression of IκBα in the macrophages. RR treatment reduced the LPS-induced phosphorylation of IKK/IκBα/p65 and suppressed IκBα degradation (**Figure 5C**). Immunofluorescent imaging study also showed that RR treatment alleviated the LPS-induced p65 translocation into the nucleus in the RAW264.7 macrophages (**Figure 5D**). These results together suggest that RR could inhibit the activation of NF-κB signaling and the expressions of iNOS and NADPH oxidase in LPS-activated macrophages.

RR Has Neuroprotective Effects on ONOO⁻ Challenged SH-SY5Y Cells

We finally addressed whether RR could have neuroprotective effects in the ONOO⁻-treated SH-SY5Y cells. SIN-1, a ONOO⁻ donor, was employed to induce nitration damage on the cells. Immunoblotting analysis revealed that SIN-1 treatment up-regulated the expressions of 3-NT and Bax in the cells whereas RR treatment inhibited the increase of 3-NT and Bax (**Figure 6A**). Immunofluorescent study revealed that RR treatment reduced HKYellow-AM positive staining cells in the cultured SHSY5Y cells treated by SIN-1 (**Figure 6B**). We then investigated the effects of RR on the macrophage-derived inflammatory challenge. To mimic the inflammatory environment, conditioned medium

(CM) was collected from LPS-stimulated macrophages for 30 min, which contained inflammatory cytokines or free radicals (Vijayan et al., 2017). Then, MTT assay was conducted to test cell viability in the SH-SY5Y cells treated with RR or vehicle under the incubation with conditioned or normal medium. The protocol was described in **Figure 6C**. As showed in **Figure 6D**, RR treatment dose-dependently increased the cell viability in the SH-SY5Y cells. These results suggest that RR had neuroprotective effects against ONOO⁻ induced neuronal cell death.

DISCUSSION

To our knowledge, this is the first report to directly demonstrate the production of ONOO⁻ in the CNS of EAE mouse model. Furthermore, for the first time, we revealed that RR could effectively suppress EAE and its underlying mechanisms are related to its anti-inflammatory and antioxidant properties via attenuating ONOO⁻-induced nitritative stress. Our study sheds a novel insight into the underlying mechanisms of MS and provides a cue for drug discovery in the MS treatment.

Oxidative/nitritative stress is intimately associated with inflammation and immunoregulation in MS pathogenesis, resulting in demyelination, axonal degradation and neuron apoptosis (Li et al., 2011). Peroxynitrite contributes to oxidative/nitritative damage in MS pathology (Smith et al., 1999). Increased 3-NT was found in serum and CSF of

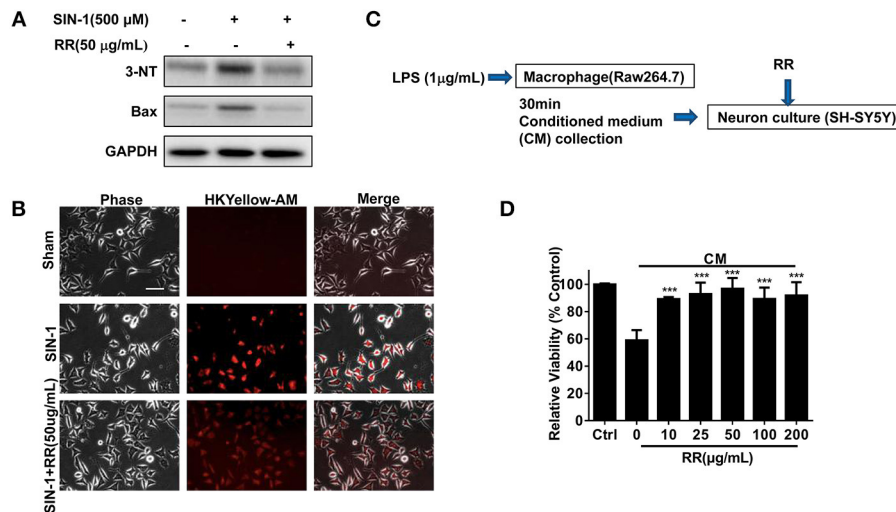


FIGURE 6 | RR protected neurons from nitritative or inflammatory cytotoxicity *in vitro*. SH-SY5Y cells were pre-treated with RR extract (50 μg/mL) or sham for 1 h, followed by 500 μM ONOO⁻ donor SIN-1 for 1 h. The expressions of 3-NT and Bax were analyzed by western blot analysis (A). ONOO⁻ levels in SIN-1 stimulated SH-SY5Y cells were detected using HKYellows-AM probe by immunofluorescent assay (scale bar, 20 μm) (B). (C) The flow chart of SH-SY5Y cells under the challenge of conditioned medium (CM), mimicking inflammatory environments. Using MTT method, the viabilities of SH-SY5Y cell treated with different concentrations of RR were measured in CM or normal medium as control (D). ****P* < 0.001.

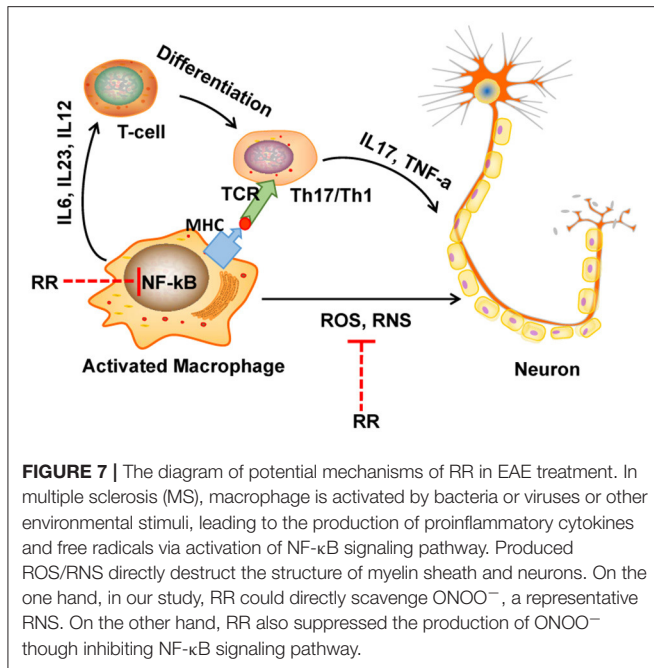
MS patients (Dujmovic et al., 2009) as well as EAE mice (Bolton et al., 2008). However, with high activity and short lifespan, ONOO⁻ is difficult to be accurately detected in biological systems. Current knowledge about the roles of ONOO⁻ in MS pathology is mainly obtained from indirect evidence. It is desirable to obtain direct evidence to detect ONOO⁻ production in MS/EAE pathogenesis. In the present study, by using HKYellows-AM, we directly visualized the production of ONOO⁻ in the spinal cords of EAE mice, supporting the role of ONOO⁻ in the MS/EAE pathogenesis.

To explore the potential effects of RR against MS pathology, we made a RR extraction with restrictive protocol and conducted quality control study. We established two reliable qualitative and quantitative methods for quality control of RR by using LCMS-IT-TOF or HPLC-DAD systems. Total 24 compounds were identified. Particularly, Catalpol showed to ameliorate pathological process of EAE mice (Yang et al., 2017; Li et al., 2018). Thus, we quantitatively detected the content of Catalpol as mark compound for quality control. It is valuable to further identify other bioactive components in the RR extract related to the protection against EAE pathogenesis.

In pharmacological studies, RR extract alleviated the disease severity and progress of the EAE mice in both prophylactic and therapeutic strategy, indicating the value of RR for multiple sclerosis treatment. Previous studies showed that RR had anti-inflammatory and neuroprotective effects on systematic autoimmune diseases and its antioxidant properties might contribute to its pharmacological actions (Li et al., 2005; Tian et al., 2006). Herein, we detected the effects of RR extract

on scavenging ONOO⁻ and inhibiting tyrosine nitration in the spinal cords of EAE mice by using HKYellows-AM probe and 3-NT detection respectively. RR showed its ONOO⁻ scavenging effects and inhibited the expression of 3-NT in the spinal cords of EAE mice at 18 dpi, the peak time of EAE. RR extract also inhibited the expressions of NADPH oxidase subunit p47^{phox}, and p67^{phox} and iNOS in the spinal cords of the EAE mice. Meanwhile, RR attenuated ONOO⁻-induced nitritative damage in SH-SY5Y cells treated with SIN-1, an endogenous ONOO⁻ donor via producing NO and O₂^{•-} to generate ONOO⁻. In addition, to avoid the artificial results from other free radicals and observe the effects of RR extract on ONOO⁻-induced nitritative damage directly, we also conducted the experiments by using exogenous synthesized ONOO⁻ and PDC as a positive control. RR treatment inhibited the apoptosis of neurons via its ONOO⁻ scavenging properties (Supplementary Figure 1). These results indicate that RR not only have direct ONOO⁻ scavenging effects but also could suppress the production of ONOO⁻ in the EAE mice. Additionally, oxidative/nitritative stress causes mitochondrial dysfunction and amplifies the oxidative/nitritative injury (Facecchia et al., 2011). Thus, we observed the morphology of mitochondria in both *in vivo* and *in vitro* experiments (Supplementary Figure 2). RR protected from mitochondrial fragmentation in the CNS of the EAE mice and the cultured SH-SY5Y cells challenged by ONOO⁻. Thus, RR extract has strong neuroprotective effects against EAE pathogenesis possibly via scavenging ONOO⁻ and inhibiting ONOO⁻-mediated neurotoxicity.

Macrophage is the major producer of ROS/RNS, contributing to oxidative/nitritative damages in MS/EAE (Nikić et al., 2011).



CD4⁺ helper T cells are crucially involved in the progressions of various autoimmune diseases including MS and EAE (Zhu et al., 2010; Mills, 2011). To investigate the anti-inflammatory effects of RR, we isolated MNCs from the brains and spinal cords of EAE mice at 30 dpi and analyzed the infiltrations of T-cells and macrophages/microglia in the lesions. RR dramatically decreased the rates of CD3⁺ T cells and CD11b⁺ CD45^{high} macrophages in the cerebral parenchyma and white matter of spinal cords in EAE mice. Meanwhile, NF-κB plays an important roles in the inflammatory and oxidative damages in EAE/MS pathology (Mc Guire et al., 2013). Activated NF-κB pathway stimulates macrophages to secrete proinflammatory factors and produce ROS and RNS (Glass et al., 2010) whereas NF-κB pathway is positive-feedback modulated by ROS/RNS (Zhang et al., 2016). Our data revealed that RR inhibited the expression of the phosphorylated IKKα/β, IκBα and p65 in splenocytes isolated from the spleens of EAE mice with dominated macrophages and lymphocytes. These results suggest that RR could inhibit NF-κB signaling in immune cells of the EAE mice. The immunosuppressing effects of RR on EAE pathology are valuable to be further investigated. The potential roles of RR in modulations of immune system and the microenvironment for the release of proinflammatory cytokines could be a potential direction for further investigation.

Of note, the RR extract contains multiple ingredients in which 24 compounds were identified in this study. Among them, Catalpol is a major component identified in RR extract. Catalpol effectively inhibited NF-κB signaling, reduced NO and ROS production and attenuated LPS-induced macrophages activation and neurotoxicity in mesencephalic neuron-glia cultures (Tian et al., 2006). Catalpol attenuated cognitive

impairment and protected hippocampal CA1 region neuronal cell death from oxidative/nitrative injury (Li et al., 2004, 2005). Catalpol treatment ameliorated the pathogenesis of EAE (Yang et al., 2017; Li et al., 2018). Thus, we used Catalpol as bioactive mark compound for the quality control of the RR extract. With 24 identified compounds and other potential unidentified compounds in the RR extract, we should further explore other bioactive compounds and their corresponding molecular targets contributing to the antioxidant and anti-inflammatory activities for ameliorating the pathogenesis of EAE. Importantly, given that the pathogenesis of MS involves a complex network of multiple factors or multiple signaling pathways, the neuroprotective effects of RR extract on MS/EAE pathogenesis could be achieved by the synergistic actions of multiple compounds for network regulations to the multiple molecular targets involved. Herbal medicine or TCM formulas with multiple compound may be more effective to modulate immune systems than the therapeutic strategy of single compound or drug development based on one target approach in MS treatment.

In conclusion, RR extract could attenuate the progress and severity of EAE through its anti-inflammatory and antioxidant effects as summarized in **Figure 7**. The underlying mechanisms could be attributed to the ONOO⁻ scavenging activity and the suppression of macrophages-derived nitrative stress in the CNS of EAE mice via inhibiting NF-κB signaling and iNOS, NADPH oxidase. Hence, this study provides a cue to further explore the bioactive compounds of RR and their molecular targets for MS treatment.

AUTHOR CONTRIBUTIONS

WL performed most of the experiments, analyzed the, data and wrote the manuscript. HW helped conducting animal experiments and analyzing data, and CG assisted in capturing images. DaY developed and supplied the ONOO⁻ detection probe, HKyellow-AM. DeY contributes to the quality control study. JS designed and supervised the research, revised the manuscript, and provided funding. All authors have read and agreed with the manuscript.

ACKNOWLEDGMENTS

This study is supported Research Grants Council AoE/P-705/16 grant and RGC GRF grant (No. 17118514), Hong Kong. We thank Faculty Core Facility, Li Ka Shing Faculty of Medicine, the University of Hong Kong to supply Carl Zeiss LSM 780/800 for capturing confocal fluorescent images and BD LSR Fortessa for flow cytometry assay.

SUPPLEMENTARY MATERIAL

The Supplementary Material for this article can be found online at: <https://www.frontiersin.org/articles/10.3389/fphys.2018.00864/full#supplementary-material>

REFERENCES

- Bishop, A., Hobbs, K. G., Eguchi, A., Jeffrey, S., Smallwood, L., Pennie, C., et al. (2009). Differential sensitivity of oligodendrocytes and motor neurons to reactive nitrogen species: implications for multiple sclerosis. *J. Neurochem.* 109, 93–104. doi: 10.1111/j.1471-4159.2009.05891.x
- Bolton, C., Scott, G. S., Smith, T., and Flower, R. J. (2008). The acute and chronic phases of chronic relapsing experimental autoimmune encephalomyelitis (CR EAE) are ameliorated by the peroxynitrite decomposition catalyst, 5,10,15,20-tetrakis(4-sulfonatophenyl) porphyrinatoiron (III) chloride, (FeTPPS). *Eur. J. Pharmacol.* 601, 88–93. doi: 10.1016/j.ejphar.2008.10.029
- Cross, A. H., Manning, P. T., Stern, M. K., and Misko, T. P. (1997). Evidence for the production of peroxynitrite in inflammatory CNS demyelination. *J. Neuroimmunol.* 80, 121–130. doi: 10.1016/S0165-5728(97)00145-8
- Dujmovic, I., Pekmezovic, T., Obrenovic, R., Nikolic, A., Spasic, M., Mostarica Stojkovic, M., et al. (2009). Cerebrospinal fluid and serum uric acid levels in patients with multiple sclerosis. *Clin. Chem. Lab. Med.* 47, 848–853. doi: 10.1515/CCLM.2009.192
- Dunham, J., Bauer, J., Campbell, G. R., Mahad, D. J., van Driel, N., van der Pol, S. M. A. et al. (2017). Oxidative injury and iron redistribution are pathological hallmarks of marmoset experimental autoimmune encephalomyelitis. *J. Neuropathol. Exp. Neurol.* 76, 467–478. doi: 10.1093/jnen/nlx034
- Facecchia, K., Fochesato, L. A., Ray, S. D., Stohs, S. J., and Pandey, S. (2011). Oxidative toxicity in neurodegenerative diseases: role of mitochondrial dysfunction and therapeutic strategies. *J. Toxicol.* 2011:683728. doi: 10.1155/2011/683728
- Glass, C. K., Saijo, K., Winner, B., Marchetto, M. C., and Gage, F. H. (2010). Mechanisms underlying inflammation in neurodegeneration. *Cell* 140, 918–934. doi: 10.1016/j.cell.2010.02.016
- Gong, J., Sun, F., Li, Y., Zhou, X., Duan, Z., Duan, F., et al. (2015). Momordica charantia polysaccharides could protect against cerebral ischemia/reperfusion injury through inhibiting oxidative stress mediated c-Jun N-terminal kinase 3 signaling pathway. *Neuropharmacology* 91, 123–134. doi: 10.1016/j.neuropharm.2014.11.020
- Jack, C., Antel, J., Bruck, W., and Kuhlmann, T. (2007). Contrasting potential of nitric oxide and peroxynitrite to mediate oligodendrocyte injury in multiple sclerosis. *Glia* 55, 926–934. doi: 10.1002/glia.20514
- Kim, H., Lee, E., Lee, S., Shin, T., Kim, Y., and Kim, J. (1998). Effect of *Rehmannia glutinosa* on immediate type allergic reaction. *Int. J. Immunopharmacol.* 20, 231–240. doi: 10.1016/S0192-0561(98)00037-X
- Kim, H. M., An, C. S., Jung, K. Y., Choo, Y. K., Park, J. K., and Nam, S. Y. (1999). *Rehmannia glutinosa* inhibits tumor necrosis factor- α and interleukin-1 secretion from mouse astrocytes. *Pharmacol. Res.* 40, 171–176. doi: 10.1006/phrs.1999.0504
- Lassmann, H., and J. van Horsen. (2011). The molecular basis of neurodegeneration in multiple sclerosis. *FEBS Lett.* 585, 3715–3723. doi: 10.1016/j.febslet.2011.08.004
- Lau, T. W., Lam, F. F., Lau, K. M., Chan, Y. W., Lee, K. M., Sahota, D. S., et al. (2009). Pharmacological investigation on the wound healing effects of Radix Rehmanniae in an animal model of diabetic foot ulcer. *J. Ethnopharmacol.* 123, 155–162. doi: 10.1016/j.jep.2009.02.010
- Lee, B., Shim, I., Lee, H., and Hahm, D. H. (2011). *Rehmannia glutinosa* ameliorates scopolamine-induced learning and memory impairment in rats. *J. Microbiol. Biotechnol.* 21, 874–883. doi: 10.4014/jmb.1104.04012
- Li, D. Q., Duan, Y. L., Bao, Y. M., Liu, C. P., Liu, Y., and An, L. J. (2004). Neuroprotection of catalpol in transient global ischemia in gerbils. *Neurosci. Res.* 50, 169–177. doi: 10.1016/j.neures.2004.06.009
- Li, D. Q., Li, Y., Liu, Y., Bao, Y. M., Hu, B., and An, L. J. (2005). Catalpol prevents the loss of CA1 hippocampal neurons and reduces working errors in gerbils after ischemia-reperfusion injury. *Toxicol.* 46, 845–851. doi: 10.1016/j.toxicol.2004.09.007
- Li, H., Nourbakhsh, B., Ciric, B., Zhang, G. X., and Rostami, A. (2010a). Neutralization of IL-9 ameliorates experimental autoimmune encephalomyelitis by decreasing the effector T cell population. *J. Immunol.* 185, 4095–4100. doi: 10.4049/jimmunol.1000986
- Li, Q., Yang, T., Guo, A. C., and Fan, Y. P. (2018). Role of catalpol in ameliorating the pathogenesis of experimental autoimmune encephalomyelitis by increasing the level of noradrenaline in the locus coeruleus. *Mol. Med. Rep.* 17, 4163–4172. doi: 10.3892/mmr.2018.8378
- Li, S. L., Song, J. Z., Qiao, C. F., Zhou, Y., Qian, K., Lee, K. H., et al. (2010b). A novel strategy to rapidly explore potential chemical markers for the discrimination between raw and processed Radix Rehmanniae by UHPLC-TOFMS with multivariate statistical analysis. *J. Pharm. Biomed. Anal.* 51, 812–823. doi: 10.1016/j.jpba.2009.10.002
- Li, S., Vana, A. C., Ribeiro, R., and Zhang, Y. (2011). Distinct role of nitric oxide and peroxynitrite in mediating oligodendrocyte toxicity in culture and in experimental autoimmune encephalomyelitis. *Neuroscience* 184, 107–119. doi: 10.1016/j.neuroscience.2011.04.007
- Liu, Y., Zhao, H., Zhang, J., Zhang, P., Li, M., Qi, F., et al. (2012). The regulatory effect of liuwei dihuang pills on cytokines in mice with experimental autoimmune encephalomyelitis. *Am. J. Chin. Med.* 40, 295–308. doi: 10.1142/S0192415X12500231
- Liu, Z., Lou, Z., Ding, X., Li, X., Qi, Y., Zhu, Z., et al. (2013). Global characterization of neutral saccharides in crude and processed Radix Rehmanniae by hydrophilic interaction liquid chromatography tandem electrospray ionization time-of-flight mass spectrometry. *Food Chem.* 141, 2833–2840. doi: 10.1016/j.foodchem.2013.04.114
- Mc Guire, C., Prinz, M., Beyaert, R., and G. van Loo. (2013). Nuclear factor kappa B (NF- κ B) in multiple sclerosis pathology. *Trends Mol. Med.* 19, 604–613. doi: 10.1016/j.molmed.2013.08.001
- Mills, K. H. (2011). TLR-dependent T cell activation in autoimmunity. *Nat. Rev. Immunol.* 11, 807–822. doi: 10.1038/nri3095
- Nikić, I., Merkle, D., Sorbara, C., Brinkoetter, M., Kreuzfeldt, M., Bareyre, F. M., et al. (2011). A reversible form of axon damage in experimental autoimmune encephalomyelitis and multiple sclerosis. *Nat. Med.* 17, 495–499. doi: 10.1038/nm.2324
- Oh, K. O., Kim, S. W., Kim, J. Y., Ko, S. Y., Kim, H. M., Baek, J. H., et al. (2003). Effect of *Rehmannia glutinosa* Libosch extracts on bone metabolism. *Clin. Chim. Acta* 334, 185–195. doi: 10.1016/S0009-8981(03)00238-9
- Peng, T., Chen, X., Gao, L., Zhang, T., Wang, W., Shen, J., et al. (2016). A rationally designed rhodamine-based fluorescent probe for molecular imaging of peroxynitrite in live cells and tissues. *Chem. Sci.* 7, 5407–5413. doi: 10.1039/C6SC00012F
- Smith, K. J., Kapoor, R., and Felts, P. A. (1999). Demyelination: the role of reactive oxygen and nitrogen species. *Brain Pathol.* 9, 69–92. doi: 10.1111/j.1750-3639.1999.tb00212.x
- Song, L., Zhou, Q. H., Wang, H. L., Liao, F. J., Hua, L., Zhang, H. F., et al. (2017). Chinese herbal medicine adjunct therapy in patients with acute relapse of multiple sclerosis: a systematic review and meta-analysis. *Complement. Ther. Med.* 31, 71–81. doi: 10.1016/j.ctim.2017.02.004
- Sung, Y. Y., Yoon, T., Jang, J. Y., Park, S. J., and Kim, H. K. (2011). Topical application of *Rehmannia glutinosa* extract inhibits mite allergen-induced atopic dermatitis in NC/Nga mice. *J. Ethnopharmacol.* 134, 37–44. doi: 10.1016/j.jep.2010.11.050
- Thompson, A. J., Toosy, A. T., and Ciccarelli, O. (2010). Pharmacological management of symptoms in multiple sclerosis: current approaches and future directions. *Lancet Neurol.* 9, 1182–1199. doi: 10.1016/S1474-4422(10)70249-0
- Tian, Y. Y., An, L. J., Jiang, L., Duan, Y. L., Chen, J., and Jiang, B. (2006). Catalpol protects dopaminergic neurons from LPS-induced neurotoxicity in mesencephalic neuron-glia cultures. *Life Sci.* 80, 193–199. doi: 10.1016/j.lfs.2006.09.010
- Vijayan, V., Srinu, T., Karnati, S., Garikapati, V., Linke, M., Kamalyan, L., et al. (2017). A new immunomodulatory role for peroxisomes in macrophages activated by the TLR4 ligand lipopolysaccharide. *J. Immunol.* 198, 2414–2425. doi: 10.4049/jimmunol.1601596
- Wu, H., Deng, R., Chen, X., Wong, W. C., Chen, H., Gao, L., et al. (2016). Caveolin-1 is critical for lymphocyte trafficking into central nervous system during experimental autoimmune encephalomyelitis. *J. Neurosci.* 36, 5193–5199. doi: 10.1523/JNEUROSCI.3734-15.2016
- Xie, Q. W., Kashiwabara, Y., and Nathan, C. (1994). Role of transcription factor NF- κ B/Rel in induction of nitric oxide synthase. *J. Biol. Chem.* 269, 4705–4708.
- Xu, J. D., Mao, Q., Shen, H., Zhu, L. Y., Li, S. L., and Yan, R. (2013). Ultra-high performance liquid chromatography coupled with photo-diode array and quadrupole/time-of-flight mass spectrometry based chemical

- profiling approach to evaluate the influence of preparation methods on the holistic quality of Qiong-Yu-Gao, a traditional complex herbal medicine. *J. Chromatogr. A* 1304, 154–168. doi: 10.1016/j.chroma.2013.07.023
- Yang, T., Zheng, Q., Wang, S., Fang, L., Liu, L., Zhao, H., et al. (2017). Effect of catalpol on remyelination through experimental autoimmune encephalomyelitis acting to promote Olig1 and Olig2 expressions in mice. *BMC Complement. Altern. Med.* 17:240. doi: 10.1186/s12906-017-1642-2
- Yu, H. H., Seo, S. J., Kim, Y. H., Lee, H. Y., Park, R. K., So, H. S., et al. (2006). Protective effect of *Rehmannia glutinosa* on the cisplatin-induced damage of HEI-OC1 auditory cells through scavenging free radicals. *J. Ethnopharmacol.* 107, 383–388. doi: 10.1016/j.jep.2006.03.024
- Zhang, J., Wang, X., Vikash, V., Ye, Q., Wu, D., Liu, Y., et al. (2016). ROS and ROS-mediated cellular signaling. *Oxid. Med. Cell. Longev.* 2016:4350965. doi: 10.1155/2016/4350965
- Zhu, J., Yamane, H., and Paul, W. E. (2010). Differentiation of effector CD4T cell populations (*). *Annu. Rev. Immunol.* 28, 445–489. doi: 10.1146/annurev-immunol-030409-101212

Conflict of Interest Statement: The authors declare that the research was conducted in the absence of any commercial or financial relationships that could be construed as a potential conflict of interest.

Copyright © 2018 Li, Wu, Gao, Yang, Yang and Shen. This is an open-access article distributed under the terms of the Creative Commons Attribution License (CC BY). The use, distribution or reproduction in other forums is permitted, provided the original author(s) and the copyright owner(s) are credited and that the original publication in this journal is cited, in accordance with accepted academic practice. No use, distribution or reproduction is permitted which does not comply with these terms.